Removal of As(III) using a natural laterite fixed-bed column intercalated with activated carbon: solving the clogging problem to achieve better performance

Régie Dimanche OUEDRAOGO , Corneille BAKOUAN , Abdoul Karim Sakira , Brahima SORGHO , Boubié GUEL * , Issa Touridomon SOMÉ , Anne-Lise HANTSON , Eric ZIEMONS , Dominique MERTENS , Philippe HUBERT , Jean-Michel Kauffmann

Posted Date: 14 September 2023

doi: 10.20944/preprints202309.0972.v1

Keywords: Laterite, Balanites aegyptiaca, percolation, activated carbon, hydraulic conductivity.

Article

Removal of *As(III)* Using a Natural Laterite Fixed-Bed Column Intercalated with Activated Carbon: Solving the Clogging Problem to Achieve Better Performance

Régie Dimanche OUEDRAOGO [1], Corneille BAKOUAN [1,2,4], SAKIRA Abdoul Karim [3,6], Brahima SORGHO [1], Boubié GUEL [1,*], Touridomon Issa SOMÉ [3], Anne-Lise HANTSON [4], Eric ZIEMONS [5], Dominique MERTENS [6], Philippe HUBERT [5] and Jean-Michel KAUFFMANN [6]

[1] Laboratoire de Chimie Moléculaire et des Matériaux (LC2M) /Equipe Chimie Physique et d'Electrochimie, U.F.R–SEA/Université Joseph KI-ZERBO, 03 BP 7021 Ouagadougou 03, Burkina Faso ; ouedraogoregie@gmail.com, sobrah20@yahoo.fr, boubieguel@yahoo.fr

[2] Laboratoire de Recherche et Développement (LRD)/Unité de Formation en Sciences et Technologies (UFR-ST)/ Université de Ouahigouya, 01 BP 346 Ouahigouya 01, Burkina Faso ; bakouancorneille@gmail.com

[3] Laboratoire de Chimie Analytique et de Toxicologie, Laboratoire de Toxicologie, Environnement et Santé, U.F.R–SDS/Université Joseph KI-ZERBO, 03 BP 7021 Ouagadougou 03, Burkina Faso ; karim_sakira@yahoo.fr, tsome66@gmail.com

[4] UMONS, Faculté Polytechnique, Département Génie des Procédés Chimiques et Biochimiques, Place du Parc 21, 7000 Mons, Belgique ; anne-lise.hantson@umons.ac.be

[5] Laboratoire de Chimie Analytique Pharmaceutique, VibraSante Hub, Département de Pharmacie/ Université de Liège (ULiège), Avenue Hippocrate 15, B36, 4000 Liège, Belgique ; eziemons@uliege.be, Ph.hubert@liege.be

[6] Laboratoire de Chimie Analytique Instrumentale et Bioélectrochimie, Université Libre de Bruxelles (ULB), Campus de la Plaine, CP 205/6, 1050 Bruxelles, Belgique ; dmertens@ulb.ac.be, jmkauf@ulb.ac.be

* Correspondence: boubieguel@yahoo.fr and boubie.guel@ujkz.bf; Tel. + 226 68 51 50 44.

Abstract: Natural laterite fixed-bed column intercalated with activated carbon prepared from *Balanites aegyptiaca* (BA-AC) was used for *As(III)* removal from an aqueous solution. Investigations were carried out to solve the problem of column clogging which appears during water percolation through the column. Experimental tests were conducted to evaluate the hydraulic conductivity and the effects of various parameters such as grain size, bed height, and initial *As(III)* concentration. The breakthrough increased from 15 to 85 h with the increase of the bed height from 20 to 40 cm, and decreased from 247 to 32 h with the increase of initial *As(III)* concentration from 0.5 to 2 mg/L. The permeability data showed that the fixed-bed column filled with laterites layers intercalated with activated carbon performs much better than the non-intercalated adsorbent column. The Bohart-Adams model showed that increasing the bed height induced a decrease in k_{AB} and N_0 values. The critical bed depths determined using the bed depth service time (BDST) model for *As(III)* removal were 15.23 and 7.98 cm for 1 and 20% breakthrough, respectively. The results showed that the new low-cost filtration system, based on laterite layers alternated with BA-AC layers, could be used for the treatment of arsenic-contaminated water.

Keywords: laterite; balanites aegyptiaca; percolation; activated carbon; hydraulic conductivity

1. Introduction

Environmental pollution has become a major concern nowadays. It has been reported that pollutants are generally introduced into the environment as a result of anthropogenic activities. Among them, heavy metals, such as *Cd*, *Cu*, *Hg*, *Ni*, *Zn*, and *Pb*, are known to be toxic to living organisms and to present a high potential risk to human health due to their accumulation through the food chain and the chain of anthropogenic activities **[1,2]**. Alongside these pollutants, arsenic (*As*) contamination of groundwater worldwide became a global issue in recent years **[2,3-5]**. In Burkina Faso, it was reported that ground waters in several localities were polluted by arsenic whose concentration in pit and drilling water was extremely higher than the World Health Organization

(WHO) standard value (0.01 mg/L) **[6]**. Arsenic is present in groundwater as arsenite (*As(III)*) and arsenate (*As(V)*) according to redox conditions **[7,8]**. Arsenite is more mobile and toxic than arsenate due to its reaction with -SH groups of proteins **[9]**. Long-term consumption of water contaminated with arsenic induces several types of cancer in organs, such as skin, liver and bladder **[3,8]**. Owing to its toxic effects and the context of water shortage in developing countries, it is urgent to develop a simple and suitable methodology for arsenic removal from contaminated ground waters. Among the existing technologies for pollutants removal from aqueous solutions, adsorption is mainly used because it is very simple to implement, cost-effective, and environmentally friendly **[10-13,14]**. Adsorption can be performed in batch mode as well as in fixed-bed columns. However, the fixed-bed system provides flexibility compared to the batch mode. Several works focused on column percolation adsorption techniques for the removal of organic and inorganic pollutants due to their simplicity and efficiency **[13,15-23]**. So far, various natural and synthetic adsorbents have been used for arsenic adsorption using fixed-bed column percolation **[23,24-27]**. In an effort to develop an efficient, low-cost and easily applied method, our previous research focused on *As(III)* adsorption in batch mode using local natural laterites **[28-29]**. These investigations paved the way for the first uses of local natural laterites from Burkina Faso for *As(III)* remediation from drinking water using the percolation technique. However, this technique encountered some shortcomings, in particular, the clogging of the column by small size laterite particles which can slow down the water flow through the column in the long run.

Clogging is generally defined as a process causing a drop in the performance of an adsorbent due to the deposition of suspended or dissolved materials on its outer surface or within the pores **[30]**. Clogging can be related to different modes such as cake formation and pore blockage by fine particles **[31]**. In the case of percolation through a laterite-lined column, small size laterite particles present low permeability to water, which leads to the clogging of the porous filter media.

The percolation treatment process has been improved by several authors who proposed the alternated layers method to solve shortcomings in the operating system **[32-33]**. Although many efforts are currently focused on the improvement of the percolation treatment, there is still a need for systematic and comparative works addressing the issue of column clogging by laterite particles in a fixed-bed column. The understanding of the clogging process which occurs during arsenic solution percolation constitutes the key element in our study. However, the question that rises is which adsorbent is going to be more appropriate to be intercalated between the laterite layers in view of the increase of the permeability of the filter media. Among several adsorbents which are currently used, activated carbon seems more suitable because of its high adsorption capacity, which is due to its large specific surface and the presence of surface charges induced by its chemical composition **[34-36]**. The use of available wastes as raw materials to prepare activated carbon appears as a good alternative to achieve a low-cost pollutant removal process **[35, 36]**. The first use of activated carbon prepared from *Balanites aegyptiaca* (BA) cores was reported by Maazou et al. **[37]** who showed that the prepared adsorbent allowed the removal of chromium from water. To the best of our knowledge, this is the first time that investigations are directed toward the understanding of those factors controlling the clogging problem during *As(III)* removal in a laterite fixed-bed column, with a view to getting an insight into a rational design of a new low-cost filter system based on laterite layers alternated with activated carbon layers. These carbon layers designated as BA-AC are likely to overcome the clogging problem occurring when *As(III)* solution is percolating in the fixed-bed column.

The main objectives of this study were to: (i) prepare and characterize a low-cost activated carbon material, (ii) study a new low-cost filter system based on laterite layers alternated with BA-AC layers, by focusing on the effects of operational parameters (natural laterite particles grain sizes, bed height, and initial arsenic concentration) on *As(III)* removal using breakthrough curve analysis, and (iii) correlate the experimental data with dynamic models to predict overall adsorption behaviors.

2. Materials and Methods

2.1. Materials

Preprints (www.preprints.org) | NOT PEER-REVIEWED | Posted: 14 September 2023 doi:10.20944/preprints202309.0972.v1

The laterite sample used in this study was collected in the locality of Dano, in the southwestern region of Burkina Faso, at the following coordinates 11°07'36.1" North and 3°02'39.5" West. The sample was designated as DA laterite.

The cores of *Balanites aegyptiaca*, used as raw materials, were collected from Balanites trees located in Ouagadougou, the Capital of the country. These cores were washed with plenty of water and then dried in the sun for 5 d. They were crushed using a rotary jaw crusher to hold the hull. The latter was ground using a mortar and then sieved to retain the particles whose size ranged between 1.0 and 1.5 mm.

2.2. Chemicals

All solutions used in this study were prepared with ultrapure water of resistivity 18.2 MΩ.cm. The material used to prepare the different solutions was soaked in nitric acid (5%) for at least 12 h and rinsed with ultrapure water before use. The stock solution of *As(III)* was prepared from $NaAsO_2$ (99%, Merck). All the reagents from Prolabo (HNO_3 65%, $NaOH$, HCl 37%, H_3P0_4 85%) were of analytical grade.

The 1000 mg/L arsenic (III) stock solution was prepared by dissolving an appropriate mass of $NaAsO_2$ (99%, Merck Ltd) in 1 L volume of milli-Q water. All working solutions, whose concentrations are 0.5, 1, and 2 mg/L, were obtained by dilution of the stock solution.

2.3. Experimental methods

2.3.1. Characterization of the adsorbent materials

2.3.1.1. Physical and chemical properties of the laterite sample

The characterization of the laterite sample, named DA laterite, was described in our previous paper **[28]**. We showed that it contained major phases such as quartz (SiO_2), kaolinite ($Al_2Si_2O_5(OH)_4$), hematite (Fe_2O_3), and goethite ($FeO(OH)$) **[28]**. The physical properties of DA laterite are shown in **Table 1** and its chemical composition is shown in **Table 2 [28].**

Two samples of laterite whose grain size ranged between $0.900 \leq G_1 < 1.250$ mm and $0.425 \leq G_2 < 0.900$ mm were used in order to investigate the influence of grain size on column clogging.

The free swelling index is a very important characteristic in our study because it permits to qualitatively characterize the swelling of the laterite. It was determined using a standard test. A mass m of dried laterite was placed in a graduated test tube. A quantity of distilled water was added and the whole was shaken regularly for one minute to suspend the laterite. The measurement of the height of the deposit was carried out as a function of time.

The swelling index was calculated using **Eq. (1):**

$$\boldsymbol{I_g = [(V_f - V_i)/V_i] \times 100} \quad \textbf{(1)}$$

I_g is the swelling index, V_i and V_f are respectively the initial and final volumes of DA laterite.

Table 1. Properties of DA laterite **[28].**

Properties	
pH_{PCN}	4.75
Bulk density (g/cm^3)	2.40
Anion exchange capacity (cmol.kg^{-1})	194.74
BET Surface area (m^2/g)	35.08

Table 2. Chemical composition of DA laterite **[28].**

Chemical composition (%)	
Fe_2O_3	20.40
Al_2O_3	19.10

 doi:10.20944/preprints202309.0972.v1

SiO_2	45.00
K_2O	0.36
Na_2O	0.20
TiO_2	1.40
MgO; MnO_2; BaO; CaO	Traces

2.3.1.2. Preparation and characterization of the activated carbon

Preparation of the activated carbon

The cores of *Balanites aegyptiaca* kernels, used as precursor, were impregnated in a 40 % phosphoric acid solution in the ratio of 1.5 g of acid per g of kernels. The impregnation was carried out in an oven at a temperature of 120 °C for 6 h. The impregnated grains were kept in hermetically sealed flasks until the carbonization (pyrolysis) tests **[38]**, carbonized in a furnace **(**muffle furnace model Nabertherm P330), and then fired in a borosilicate glass crucible at a temperature of 450 °C with a heating rate of 7.5 °C/min and 2 h isotherm step**.** The resulting activated carbon was cooled at room temperature in a desiccator. After acid activation, the product was washed with 0.1 mol.L^{-1} hydrochloric acid to remove the impurities. Then, the product was washed with distilled water, until a pH value of 6.5 was reached, and dried in an oven at 105°C for at least 8 h **[35, 39]**. The different steps in the synthesis of activated carbon BA-AC are shown in **Figure 1**.

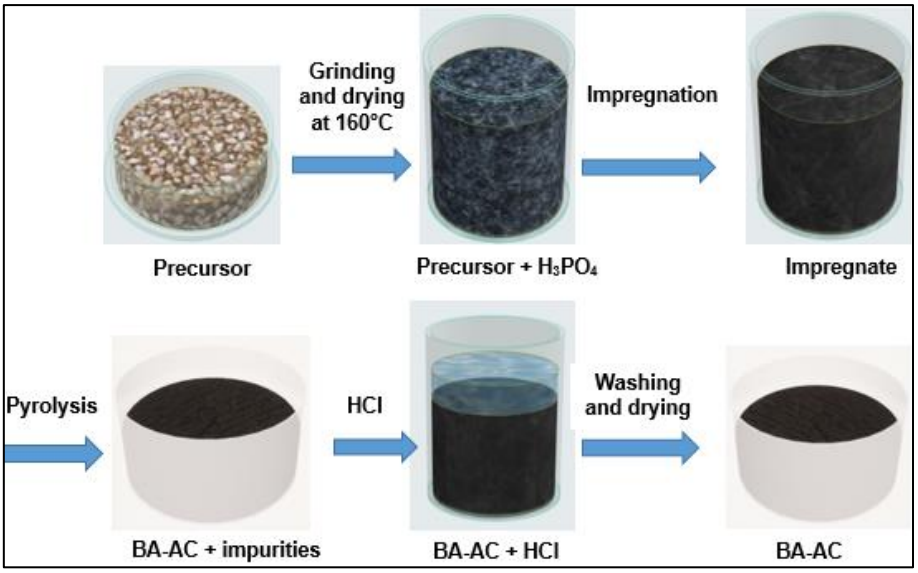

Figure 1. The steps in the synthesis of activated carbon BA-AC.

Characterization of the activated carbon

Before undertaking arsenic (III) adsorption tests, BA-AC was fully characterized by running several physicochemical measurements. The Brunauer-Emmett-Teller (BET) analysis and the Barret-Joyner-Halenda (BJH) isotherm (ASAP 2020 accelerated surface area and porosimetry system from Micromeritics Norcross GA, USA) made it possible to determine respectively the specific surface area, the pore volume and the pore size of the activated carbon BA-AC samples. The morphological characterization of the BA-AC samples was achieved by running scanning electron microscopy (SEM HITACHI SU8020 computer-controlled with the software EDX SDD, Thermo Scientific, Mons, Belgium). To characterize the adsorbent material BA-AC, X-ray powder diffraction (XRPD) was carried out on a D8 Advance Davinci Bruker X-ray generator diffractometer (working at 40 mA generator current and 40 kV generator voltage with Cu-Kα radiation (λ = 1.54060 Å)). The XRPD data were recorded at a scan speed of 0.02° s^{-1} and in the 2θ angles values ranging from 5° to 70°.

2.3.2. Fixed-bed column investigations

2.3.2.1. Column experiment setting up

Preprints (www.preprints.org) | NOT PEER-REVIEWED | Posted: 14 September 2023 doi:10.20944/preprints202309.0972.v1

The studies of the column were carried out in two steps. In the first step, a glass column with a diameter of 7 cm was packed only with DA laterite. A second column was filled with DA laterite interspersed at 25% of the total height of the bed by BA-AC distributed in five layers of equal height. For the column packed only with DA laterite, the tests were performed at different depths (20, 30, and 40 cm) and with different particle sizes ($0.900 \leq G_1 < 1.250$ mm; and $0.425 \leq G2 < 0.900$ mm). For the second column (DA laterite-BA-AC), the study was conducted at different experimental conditions, such as the effect of bed depth (20, 30, and 40 cm) and the effect of initial concentration (0.5, 1, and 2 mg/L).

The *As(III)* solutions were stored in a 20 L canister with a hand tap suitable for the rural area and introduced into the fixed-bed column in a down-flow mode through the column at a constant flow rate of 50 mL/min. This flow rate was chosen to provide a sufficient amount of effluent per minute that was acceptable on a field scale.

In order to avoid migration and floating of the adsorbents and to allow uniform distribution of the solution through the column, glass wool was placed on both sides of the column. Treated *As(III)* samples were collected at regular interval time in a 40 mL tube and analyzed by using an electrochemical method, which was developed by **Sakira et *al*. [6]**.

The column was considered to be exhausted when the effluent concentration was greater than 10 µg/L (WHO guide). All experiments were performed at room temperature. The experimental setup is represented in **Figure 2**.

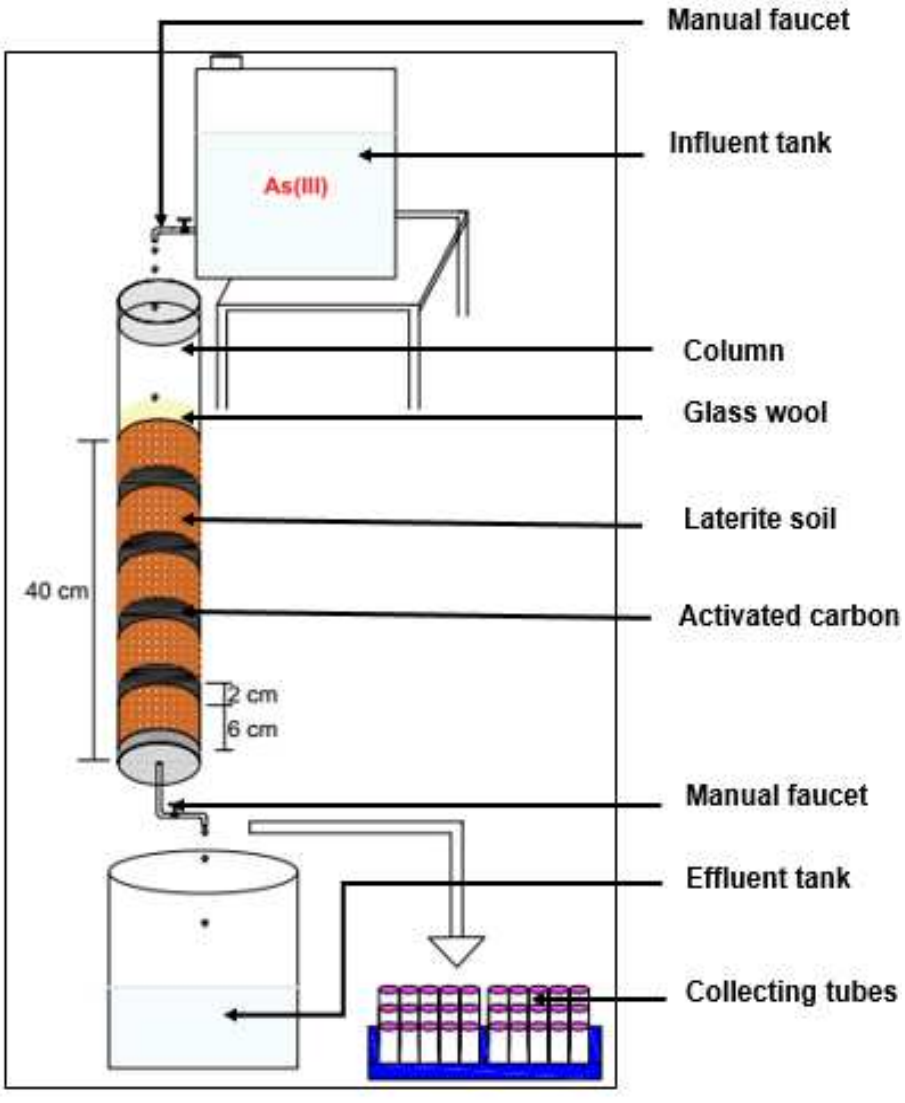

Figure 2. Experimental device for solution percolation through a natural laterite fixed-bed column alternated with activated carbon layers.

Preprints (www.preprints.org) | NOT PEER-REVIEWED | Posted: 14 September 2023 doi:10.20944/preprints202309.0972.v1

2.3.2.2. Fixed-bed column data analysis

The analysis of the column data was performed according to literature **[40].** The escape time (t_e) is defined as the point on the breakthrough curve at which adsorbate is detected at the outlet of the column, while the breakthrough time (t_p) is the point on the curve where the arsenic concentration reaches its maximum allowable value of 0.01 mg/L **[41]**. The column was considered to be exhausted when the arsenic (III) concentration at the column outlet reached the maximum allowable level (0.01 mg/L) **[42]**.

The breakthrough curve is usually expressed as $\left({}^{C_t}/_{C_0}\right)$ as a function of time or volume treated for a given bed depth.

The volume V(mL) processed can be calculated from **Eq. (2).**

$$\boldsymbol{V(\mathrm{mL}) = Q \times t_{tot}} \quad \textbf{(2)}$$

Q and t_{tot} are the volumetric flow rate (mL/min) and the total flow time (min), respectively.

The total amount of arsenic adsorbed in the column, $q_{tot}(mg)$, is calculated from the area under the breakthrough curve using **Eq. (3) [41].**

$$\boldsymbol{q_{tot}(\mathrm{mg}) = \frac{Q}{1000}\int_{t=0}^{t=tot} C_{ad}\,dt = \frac{Q}{1000}\int_{t=0}^{t=tot}(C_0 - C_t)\,dt} \quad \textbf{(3)}$$

$\boldsymbol{C_{ad}}$ is the concentration of arsenic adsorbed at time t, C_0 is the initial arsenic concentration and C_t is the arsenic concentration at time t. All concentrations are in mg/L.

The maximum equilibrium arsenic adsorption capacity of the column $q_{eq}\left({}^{mg}/_{g}\right)$ is calculated from **Eq. (4) [43].**

$$\boldsymbol{q_{eq}\left({}^{mg}/_{g}\right) = \frac{q_{tot}}{m}} \quad \textbf{(4)}$$

m is the mass (in g) of the adsorbent in the column.

The total amount of arsenic introduced into the column is calculated using **Eq.(5) [41].**

$$\boldsymbol{m_{tot}\,(mg) = \frac{C_0 \times Q \times t_{tot}}{1000}} \quad \textbf{(5)}$$

The percentage of arsenic removed $R(\%)$ can be obtained from **Eq. (6) [41]**.

$$\boldsymbol{R(\%) = \frac{q_{tot}}{m_{tot}} \times 100} \quad \textbf{(6)}$$

Bohart-Adams model and Bed Depth Service Time model (BDST)

In order to facilitate the scaling up of the process without being too expensive, to predict the results instead of carrying them out in the laboratory, and to avoid important delays in the realization of the experiments, we have modelled the column using two theoretical models, namely the Bohart-Adams model and the Bed Depth Service Time model (BDST).

Bohart-Adams model

The Bohart-Adams model is described by **Eq. (7) [42]:**

$$\boldsymbol{ln\left(\frac{C_t}{C_0}\right) = \mathrm{K_{AB}} \times C_0 \times t - \mathrm{K_{AB}} \times N_0 \times \left(\frac{\mathrm{Z}}{U_0}\right)} \quad \textbf{(7)}$$

C_0 (mg/L) is the initial arsenic concentration, C_t (mg/L) is the arsenic concentration at the column outlet at time t (h), k_{AB} is the kinetic constant $(\frac{L}{mg}.h)$ of Bohart-Adams , N_0 is the saturation concentration or mass capacity (mg/L), Z is the height of the fixed-bed column (cm) and U_o is the surface velocity (cm/h) defined as the ratio of the volumetric flow rate Q (cm^3/h) and the cross-sectional area A (cm^2) of the bed.

The Bed Depth Service Time model (BDST)

The Bed Depth Service Time model (BDST) is represented by equations **(8)** and **(9) [42]**:

Preprints (www.preprints.org) | NOT PEER-REVIEWED | Posted: 14 September 2023 doi:10.20944/preprints202309.0972.v1

$$ln\left(\frac{C_0}{C_t}-1\right) = K_{AB}\times C_0\times t - K_{AB}\times N_0\times\left(\frac{Z}{U_0}\right) \quad (8)$$

Hence $t = \frac{N_0}{C_0U_0}Z - \left(\frac{1}{C_0K_{AB}}\right)ln\left(\frac{C_0}{C_t}-1\right)$ (9)

Where C_0 (mg/L) is the initial solute concentration, C_t (mg/L) is the desired solute concentration at a defined breakthrough time, K_{AB} the adsorption rate constant (L/(mg h)) with h in hours, N_0 the adsorption capacity (mg/L), Z the column depth (cm) and t is the operating time of the column (h).

By fixing **t = 0** and solving **Eq. (9)**, we obtain **Eq. (10)**:

$$Z_0 = \left(\frac{U_0}{N_0K_{AB}}\right)\ln\left(\frac{C_0}{C_t}-1\right)$$

(10)

In this technique, called the BDST (bed depth service time) approach, the Bohart-Adams equation is expressed by **Eq. (11 -13) [42]:**

$$t = az + b$$

(11)

$$a = \frac{N_0}{C_0U_0}$$

(12)

$$b = \left(\frac{1}{C_0K_{AB}}\right)ln\left(\frac{C_0}{C_t}-1\right)$$

(13)

This equation allows us to determine the theoretical operating times of the column by studying the influence of the bed depth.

2.3.3. Hydraulic conductivities

The characterization of both intercalated and non-intercalated laterite can be done by investigating the modification of a specific physical property. We have chosen the hydraulic conductivity as its measurement can be carried out at a low-cost and is easy to implement. The hydraulic conductivities of non-intercalated laterite bed and intercalated laterite bed were determined by the Darcy's law, using a constant head permeability meter with 20 cm height (L) material layer, and 7 cm diameter. The water was allowed to flow downwards through the material. The flow rate (Q) was measured. The hydraulic conductivity or permeability coefficient K (cm/s) was determined using the following **Eq. (14) [44].**

$$K = \frac{Q.L}{A.\Delta H}$$

(14)

where Q is the flow rate (cm³/s); K is the saturated hydraulic conductivity or permeability coefficient (cm/s); ΔH is hydraulic head pressure (cm); L is length of the material layer (cm); A is the cross-sectional area of the column (cm²).

The infiltration rate of water is determined from **Eq. (15) [44].**

$$v = \frac{Q}{A} = K.i$$

(15)

i represents the imposed hydraulic gradient without unit, it is determined using **Eq.(16). [44].**

$$i = \frac{\Delta H}{L} \quad (16)$$

The measurement of the hydraulic conductivities of the non-intercalated laterite bed and intercalated laterite bed provided data which confirmed the intercalation in the fixed-bed system.

Preprints (www.preprints.org) | NOT PEER-REVIEWED | Posted: 14 September 2023 doi:10.20944/preprints202309.0972.v1

2.4. Statistical analysis

The data fitting of the percolation adsorption and the standard deviation of the free swelling index of DA laterite were carried out using Excel (version Microsoft Excel 2016). Differences were considered significant at p value < 0.05.

3. Results and discussion

3.1. Free swelling index of DA laterite

Figure 3 shows that the free swelling index increases with the depth (*Z*) of the fixed-bed column. This figure also shows that the swelling index evolves with the wetting time and it stabilizes after 24 h**.** In fact, it can be noticed that the free swelling index increases from 23.26 to 28.03% when the bed height increases from 5 to 15 cm. This increase of the swelling index is certainly due to the presence of a significant amount of swelling minerals or clayey parts. Swelling is mainly related to the mineralogical nature of the clays **[43]**.

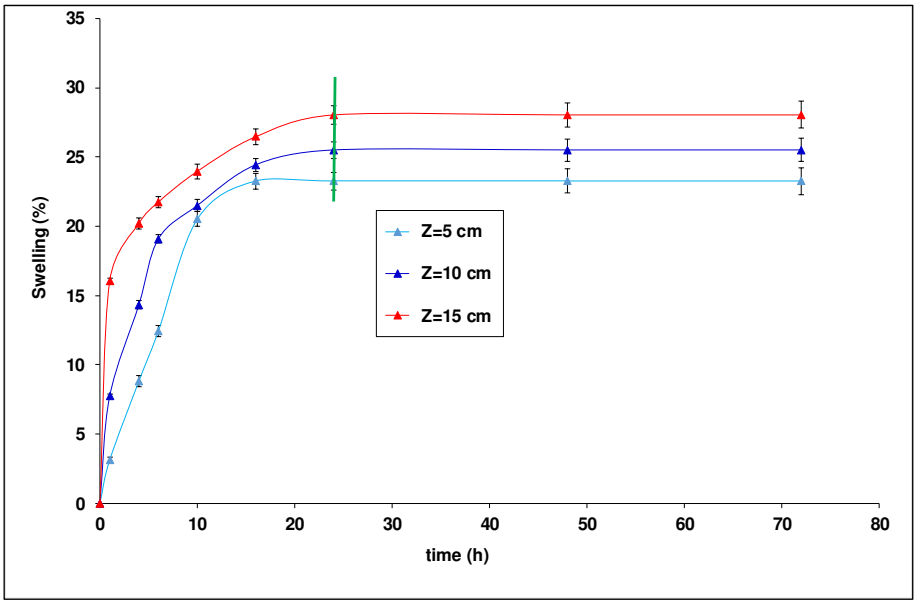

Figure 3. Free swelling index as a function of time.

3.2. Characterization of activated carbon

3.2.1. Physicochemical characteristics

The knowledge of the physicochemical characteristics of carbon (thermal and/or chemically activated) is necessary to understand many phenomena such as adsorption, desorption, ion exchange and others **[34,35].** The results of the characterization are summarized in **Table 4**. It can be noticed that the BA-AC has a suitable specific surface and porosity for the adsorption of *As(III)*. The specific surface area value of BA-AC determined by BET method is 666.464 m^2/g. This value is significantly high compared to literature-reported values, which are in the range of 520-876 m^2/g, for activated carbons synthesized from local biomasses in view of *As(III)* adsorption **[15,35,45]**. It can also be noted that BA-AC has relatively small average pore diameters (2.7834 nm), almost at the limit of micro porosity, and a large micropore volume (0.2720 cm^3/g). The size of these pores, less than 2 nm, and the small total pore volume confirm its microporous nature as defined by the International Union of Pure and Applied Chemistry (IUPAC) classification for pore size ranges **[37]**.

The iodine and methylene blue indices, used to determine the nature of the dominant pores of the activated carbon, were 15.44 mg/g and 869.95 mg/g, respectively. The highest value of the iodine index resulted from a predominance of micropores and it contributed to increase the adsorption capacity of BA-AC **[37,39]**.

Preprints (www.preprints.org) | NOT PEER-REVIEWED | Posted: 14 September 2023 doi:10.20944/preprints202309.0972.v1

Table 4. Physicochemical characteristics of activated carbon.

Parameters	Values
C (%)	80.00
Iodine number (mg/g)	869.95
Methylene blue number (mg/g)	1.32
Surface area (S_{BET}) m^2/g	666.46
Micro-pore surface area (S_{mic}) m^2/g	610.70
Total pore volume (V_p) cm^3/g	0.27
Average diameter of pore by BET nm	2.78
Average diameter of pore by BJH nm	2.97

3.2.2. Structural characteristics

The diffractogram of the activated carbon (**Figure 4**) did not show any crystalline phase. It clearly indicated that the BA-AC was characterized by an amorphous structure with no detectable crystallized species on its surface, as reported in the literature **[45, 34]**. This amorphous structure has a huge advantage regarding pollutant adsorption. Indeed, a well-prepared activated carbon consists mainly of amorphous structure, which is highly porous, exhibiting a broad range of open pore sizes of molecular dimensions, and appropriate for pollutant adsorption through column percolation. The amorphous structure was confirmed by the SEM analysis.

The SEM analysis shows the nature of the pores on the BA-AC particles surface (**Figure 5**)**.** The SEM images in **Figures 5c and 5d** are characterized by a similar porous morphology, while those in **Figures 5a and 5b** show relatively more homogeneous pores with constant diameters. Pores like capillary cracks are observed in the Figures **5a, 5b** and **5c**. These cracks have different sizes and inside the larger ones, additional cracks with smaller diameter are observed. This results indicates that BA-AC is characterized by a significant porosity and pores of different sizes **[33].**

The results of the EDX analysis provided the elemental analysis of BA-AC. It was observed that BA-AC contained mainly carbon atoms and oxygen atoms in small quantities. This result confirmed that the BA-AC was a strongly carbonaceous material with 85%. Other atoms that are present, such as oxygen 11.75%, phosphorus 2.85% and trace amounts of calcium, were either from the composition of the raw material or from the activating agent. The presence of the phosphorus atom may be a product resulting from the reaction of phosphate ions with the raw material **[7].**

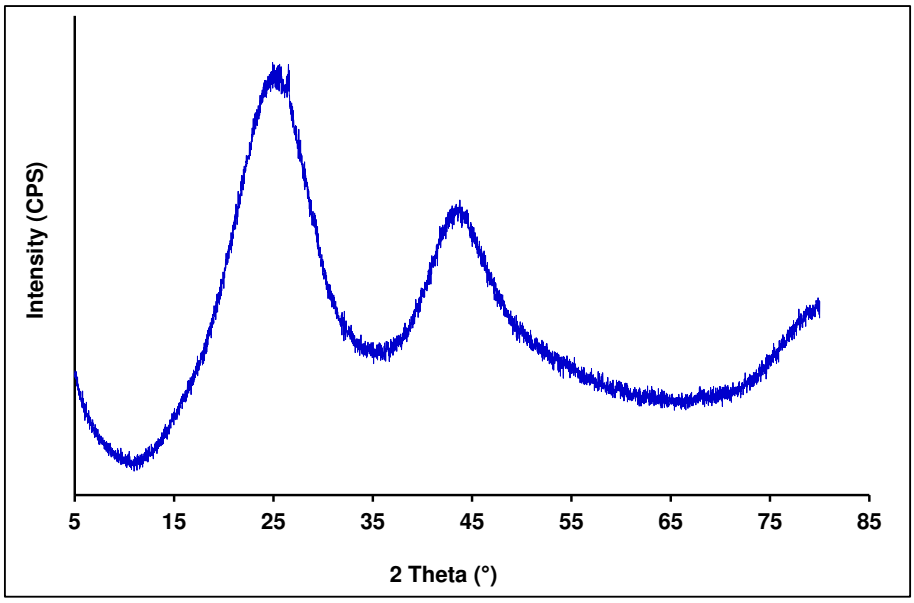

Figure 4. Diffractogram of BA-AC.

Preprints (www.preprints.org) | NOT PEER-REVIEWED | Posted: 14 September 2023 doi:10.20944/preprints202309.0972.v1

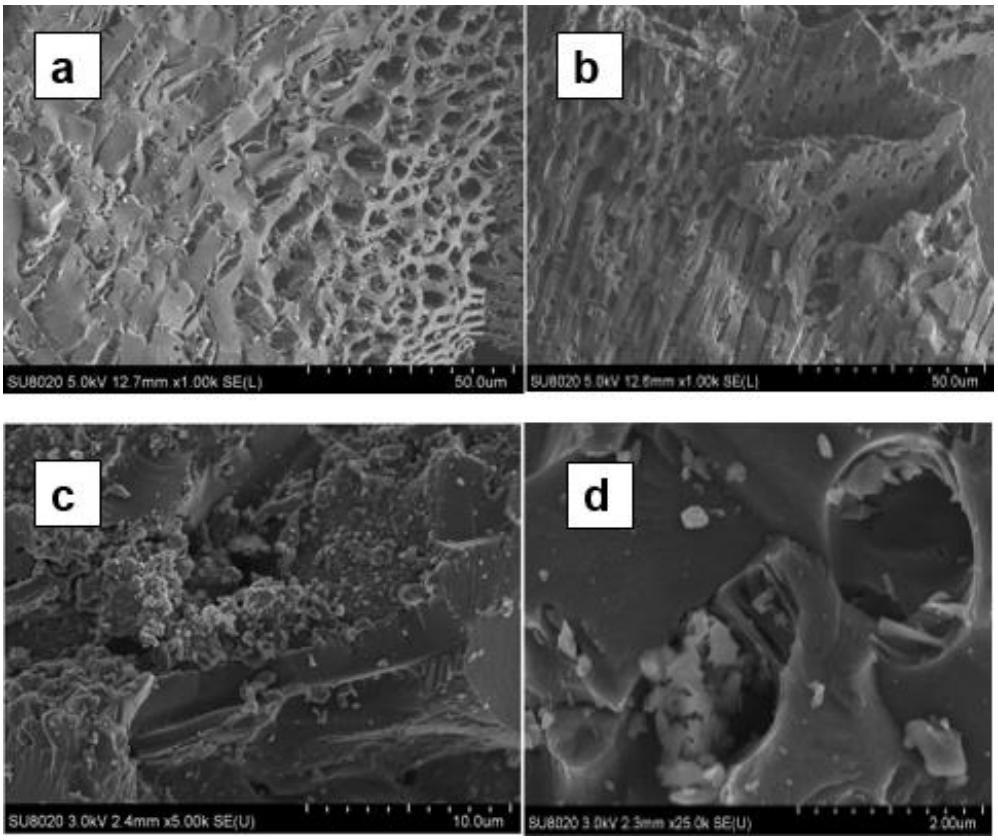

Figure 5. SEM image of BA-AC. (**a**): zoom on a grain at 50 µm, **(b**): zoom on another grain at 50 µm, (**c**): zoom on a grain at 10 µm; (**d**): zoom on a grain at 2µm.

3.3. Investigations of fixed-bed column packed with only DA laterite

3.3.1. Effect of the bed height

The appreciation of the column clogging by laterite particles as a function of the bed height was inferred from a decrease in the affluent flow rate as a function of time**. Figure 6** shows that the bed height favored the compaction of the laterite causing a risk of clogging; the higher the bed height, the higher the risk of clogging. The interruption time was defined as the time elapsed from the beginning of the percolation to clogging when the effluent stops percolating through the column. These 30 and 40 cm bed height criteria were equal to 7 and 3 h, respectively. However, with a bed height of 20 cm, the breakthrough time occurred without the clogging of the filter by laterite particles during the percolation process. Indeed, we noticed that for 30 and 40 cm, a large part of fine particles exhibited a high swelling rate compared to the one related to 20 cm **(Figure 6).** The clogging phenomenon observed for these bed heights (30 and 40 cm) could be explained by the fact that a higher bed depth favored the development of a stilling zone. The latter served as a deposition site for fine particles resulting in a decrease of the water load passing through the layers. As a matter of fact, in the case of a fixed-bed column filled with only laterite particles, the use of higher bed depths, with a view to a better adsorption capacity and a higher breakthrough time, will always encounter column clogging in the long run, in contrast to reported results in the literature **[23].** To overcome this issue of clogging occurring for high bed depths, the method of alternating layers (laterite layers alternated with activated carbon layers) was examined in the subsequent investigations.

Preprints (www.preprints.org) | NOT PEER-REVIEWED | Posted: 14 September 2023 doi:10.20944/preprints202309.0972.v1

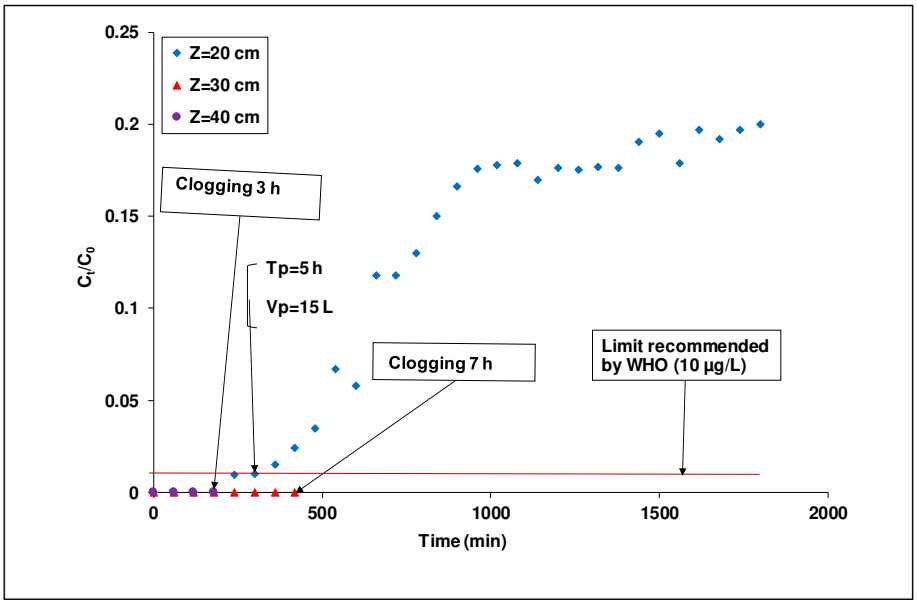

Figure 6. Breakthrough curves of *As(III)* adsorption in DA laterite packed column at different bed depths (([*As(III)*]$_i$ =1 mg/L flow rate=50 mL/min; diameter =7 cm; grain size 0.900 ≤ G ≤ 1.250 mm).

3.3.2. Effect of particle size

The study of the column clogging by laterite particles as a function of laterite particle size is illustrated in **Figure 7.** In this figure, it can be seen that the reduction of laterite particle size accentuated the column clogging by laterite particles. This can be explained by the fact that there were more fine particles in the column (0.425 ≤ G_2 < 0.900 mm) giving a high swelling rate. Because the fine laterite particles contained a significant amount of oxide Fe_2O_3 (20.4%), it seems reasonable to foresee electromagnetic phenomena that could occur between the surface of the laterite grains and the iron particles. This may generate a deposition layer by adsorption on the grains surface **[46].** These electromagnetic phenomena, occurring between the surface of the laterite grains and the iron particles, combined with the deposition of fine particles on the surface of the filtering structure were likely the cause of the progressive clogging of the interstices of the laterite layers. For an efficient operation i.e. without clogging of the filter during the percolation process, an intercalation of layers by a non-swelling adsorbent material was further considered.

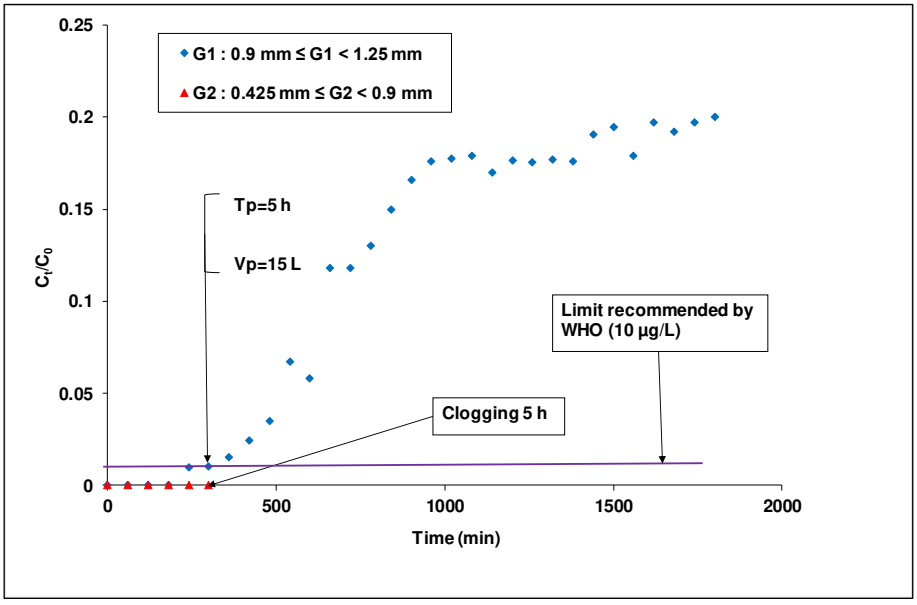

Figure 7. Breakthrough curves of *As(III)* adsorption in column packed with laterite of different particle sizes ([As(III)]$_i$ =1 mg/L, flow rate=50 mL/min; diameter =7 cm ; bed height =20 cm).

Preprints (www.preprints.org) | NOT PEER-REVIEWED | Posted: 14 September 2023 doi:10.20944/preprints202309.0972.v1

3.4. Investigations of column packed with alternated layers of laterite and activated carbon

3.4.1. Comparative study of the performance between an intercalated laterite column and a non-intercalated laterite column

Dynamic mode retention tests of arsenic (III) in the two columns, with an identical value of bed height (20 cm), gave breakthrough times of about 5 and 15 h for a column packed with only laterite and the other one packed with laterite intercalated by activated carbon, respectively **(Figure 8)**. In addition, the adsorption capacities obtained for a column packed with only laterite and the other one packed with laterite intercalated with activated carbon were 0.0173 mg/g and 0.0530 mg/g, respectively. These results confirmed that the column packed with laterite intercalated with activated carbon have a better performance than the one packed with non-intercalated laterite.

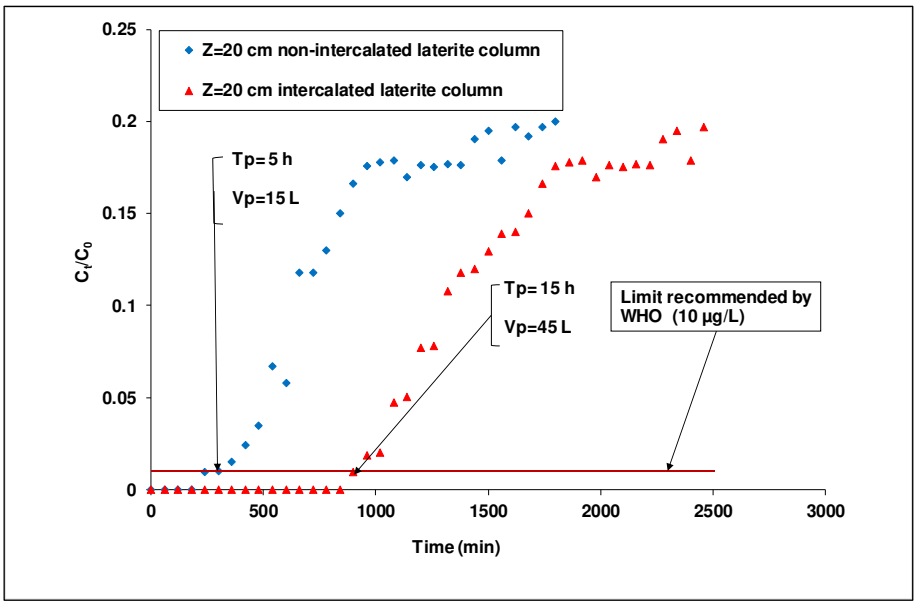

Figure 8. Comparison of the performance of an intercalated laterite column and a non-intercalated laterite column ($[As(III)]_i$ =1 mg/L, flow rate=50 mL/min; diameter =7 cm; 0.900 ≤ G ≤ 1.250 mm, bed height =20 cm).

At this step, it is worth carrying out hydraulic measurements to state why the fixed-bed column packed with intercalated adsorbents exhibits a better performance than the one with non-intercalated adsorbents. The increase of the permeability to water of the porous system when we switch from the non-intercalated adsorbent to the intercalated adsorbent will give the evidence of such a behavior. Darcy law experiment was implemented to find the hydraulic conductivity or the permeability constant (K), which stands for the porous filter ability to conduct water **[44]**. The results obtained are shown in the **Table 5.**

In **Table 5**, the permeability constants obtained for the non-intercalated laterite bed and the intercalated laterite bed are 0.0021 cm/s and 0.0044 cm/s, respectively. These values are in the same order of magnitude as those of coarse particles (10^{-3} - 10^{-1} cm/s) **[47]**. In silts and clayey sands, the hydraulic conductivity is low, varying between 10^{-7} and 10^{-3}cm/s, while in clays it varies between 10^{-11} and 10^{-7}cm/s, which makes them practically impermeable **[47]**.

It can be noted that the intercalated laterite bed system presents a significant increase in permeability due to a higher flow velocity in comparison to the non-intercalated bed system, which affected the permeability of the column. The main differences which are observed in terms of permeability values can easily be related to the performance of the two column models.

Laterite is well known as a swelling material. Basing on literature, it is also known that an intercalation of a swelling adsorbent by a non-swelling adsorbent material could improve the permeability to water of the porous filter media. As expected, the intercalated laterite bed exhibits a higher hydraulic conductivity compared to the non-intercalated laterite bed, and consequently

Preprints (www.preprints.org) | NOT PEER-REVIEWED | Posted: 14 September 2023 doi:10.20944/preprints202309.0972.v1

performs well. A higher hydraulic conductivity is linked to a higher flow rate, and a lower residence time of the water inside the porous material, diminishing the risk of clogging. The hydraulic conductivity data not only allow us to assess the intercalation formation in the fixed-bed system, but will also provide the assurance that the intercalated laterite bed method can be applied for the removal of *As(III)* without any risk of clogging. So far, no permeability data have been reported for a natural laterite fixed-bed column intercalated with activated carbon. The present investigations provide data for an appropriate justification of the modification of the porous system's permeability when the laterite bed system is intercalated by activated carbon layers.

Table 5. Physical properties of the porous filter system.

Materials	A(cm^2)	Hydraulic gradient i	Q (cm^3/s)	Hydraulic conductivity or permeability coefficient K (cm/s)
Non-intercalated laterite bed	38.4650	4.2500	0.3477	0.0021
Laterite bed intercalated with activated carbon	38.4650	4.2500	0.725	0.0044

3.4.2. Effect of the bed height on the breakthrough curve

Arsenic treatment by DA laterite packed column alternated with BA-AC was studied as a function of the bed height (20, 30 and 40 cm) in a 7 cm diameter column. A synthetic *As(III)* solution of C_0 equals to 1 mg/L was used with a flow rate set at Q equals 50 mL/min. In this study of arsenic (III) removal in dynamic mode, the breakthrough curves ($C_t/C_0 = f(t)$) were plotted to determine the breakthrough time **(Figure 9)**. Breakthrough was obtained when the arsenic concentration in the treated water was greater than or equal to the limit value (10 µg/L). The results are reported in **Table 6.**

It is noted that, contrary to the results obtained in Figure 6 where an interruption of the percolation occurs for Z equals 30 and 40 cm, the combination of the natural laterite and the activated carbon permitted to avoid the clogging. Moreover, it can be seen (**Figure 9)** that with the increase of the bed height from 20 to 40 cm, the breakthrough time raised from 15 to 85 h, resulting in an increase in the volume of the treated *As(III)* solution from 45 to 255 L. Indeed, a higher bed height contains more mass of the adsorbent, which requires a longer time to reach saturation point and thus breakthrough **[24]**. This is in line with the data of **Table 6** which indicates that the total amount of *As(III)* adsorbed increased from 44.450 to 252.450 mg when the bed height increased from 20 to 40 cm, respectively. These results highlighted the fact that at a higher bed height, the mass or adsorbent surface increases, and consequently the number of sorption sites that are likely to bind arsenic (III) increases **[23,48].** As a result, we observed a greater adsorption capacity for *As(III)* as the bed height increases **[5]**.

Preprints (www.preprints.org) | NOT PEER-REVIEWED | Posted: 14 September 2023 doi:10.20944/preprints202309.0972.v1

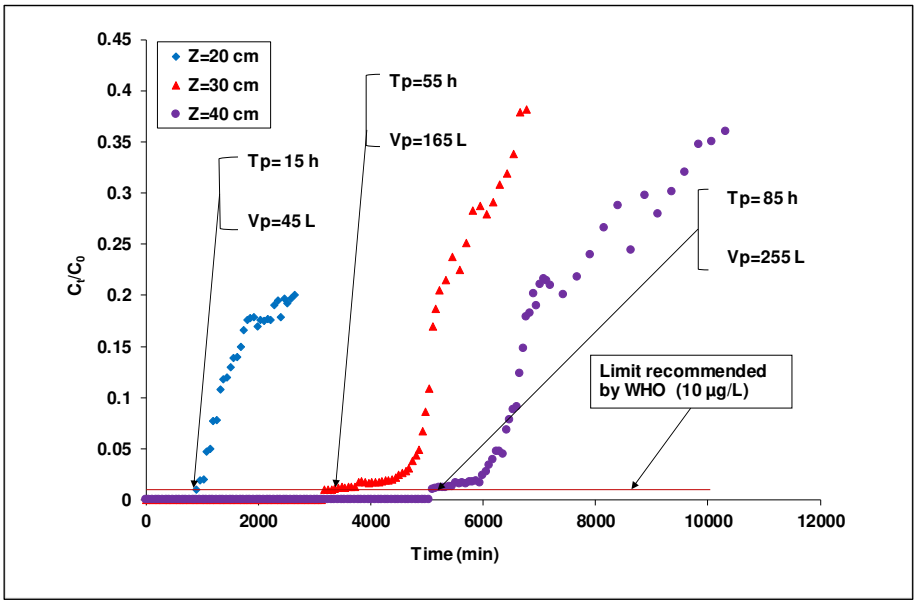

Figure 9. Breakthrough curves of *As(III)* adsorption in laterite packed column intercalated with activated carbon at different bed depths ([*As (III)*]$_i$ =1 mg/L, flow rate=50 mL/min; diameter =7 cm ; 0.900 ≤ G ≤ 1.250 mm)).

Table 6. Fixed-bed column parameters for adsorption of *As(III)* in DA laterite packed column intercalated with activated carbon at different bed depths.

Z (cm)	Mass (kg)	*tp* (min)	*Vp* (L)	Q_{tot}(mg)	Q_p(mg/g)	*R*(%)
20	0.839	900	45	44.450	0.053	99
30	1.425	3360	168	166.320	0.116	99
40	1.780	5100	255	252.450	0.141	99

3.4.3. Dynamic models

3.4.3.1. Modeling from the Bohart-Adams equations

The Bohart-Adams model was used to investigate the kinetics of arsenic removal in a column filled with DA laterite layers intercalated with BA-AC. The volumetric capacity (N_0) and the rate constant (K_{AB}) of the fixed-bed column system were determined and their values are reported in **Table 7**.

The coefficient of determination R^2 (**Table 7**) increases from 0.887 to 0.980 when the bed height *Z* increases from 20 to 40 cm. The high value of the coefficient of determination (R^2 equals 0.980 for 40 cm as bed height) indicates that at this height the Bohart-Adams model describes the experimental data satisfactorily. The increase of the bed height leads to a decrease of both K_{AB} and N_0 values, as already shown in previous investigations on *As(III)* adsorption **[43,48].** In fact, increasing the bed height resulted in an increase of the contact time of arsenic (III) species with the DA laterite layers intercalated with activated carbon, which ultimately resulted in a better efficiency of the percolation process **[24].** Thus, the decrease in rate constant from 0.0023 to 0.0015 L.mg^{-1}.min^{-1} when the bed depth increased from 20 to 40 cm suggested that the adsorption kinetics slowed down as a result of the adsorbent mass increase **[49].**

Table 7. Bohart-Adams model parameters for *As(III)* adsorption in a fixed-bed column system.

Z (cm)	Mass (kg)	N_0 (mg/L)	K_{AB} (L.mg^{-1}.mn^{-1})	R^2
20	0.8390	12.3371	0.0023	0.8874
30	1.4250	6.2693	0.0015	0.9761
40	1.7800	2.7993	0.0014	0.9809

 doi:10.20944/preprints202309.0972.v1

3.4.3.2. Application of the BDST (Bed Depth Service Time) mode

The experimental results obtained from the adsorption of *As(III)* by percolation in a column packed with DA laterite layers intercalated with BA-AC were fitted to the BDST model to determine the adsorption capacities and kinetic constants. It was previously reported that the breakthrough and saturation times corresponding to $C_t/C_0 = 0.01$ and $C_t/C_0 = 0.2$, respectively, were found to be 15 h, 55 h, and 85 h and 44 h, 87 h, and 120 h for bed depths of 20, 30, and 40 cm, respectively. **Figure 10** shows the service time versus depth plot for 1 and 20% saturation.

From the slope and intercept of the 1 and 20% saturation line shown in **Figure 10**, the design parameters N_0 and K_{AB} were determined using **Eq. (12)** and **(13)**.

In **Figure 10,** it can also be seen that when the bed depth Z increased, the breakthrough time t_p also increased. This is related to the amount of adsorbent that increased the adsorption capacity of the column. Finally, **Figure 10** shows that the variation of breakthrough time with bed depth is linear, which validates the BDST model. The BDST parameters, such as sorption rate constant (k_t), sorption capacity (N_0) and critical bed depth (Z_0) were calculated and the results are summarized in **Table 8.**

For 1 and 20% saturation, it was observed (**Table 8)** that the determination coefficient values were all high ($R^2 = 0.99$). This proves that the results were consistent with the BDST model. There was also a steady increase in the slope from 3.5 to 3.8 when the breakthrough increased from 1 to 20% and a consistent increase in the coherent dynamic adsorption capacity (N_0) from 1335.60 to 1450.0800 mg/L of *As(III)*. It is evident that after the saturation at 1%, some adsorbent active sites were still available for *As(III)* adsorption. Similar observations were also reported by **Podder et *al.*** on a fixed-bed column filled with bacterial cells immobilized on a sawdust/$MnFe_2O_4$ composite **[24]**. It was shown that the slope increased from 0.0900 to 0.4300 and from 0.105 to 0.415, for *As(III)* and *As(V)* respectively, when the breakthrough increased from 1 to 20%. It was also observed by the authors that the coherent dynamic adsorption capacity (N_0) increased from 45.216 to 216.032 mg/L and from 52.752 to 208.496 mg/L, for *As(III)* and *As(V)* removal, respectively **[24]. Goel et *al.*** also reported a slope increase from 12.50 to 35 for breakthrough values of 20-60% for the removal of lead using granular activated carbon **[50]**.

The Bohart-Adams equation (BDST theory) assumes a rectangular isotherm with a constant dynamic adsorption capacity. All of these investigations recommended that the validation of the BDST model cannot be performed by only examining the coefficient of determination (R^2). The BDST model coefficients of a smaller breakthrough can still be used to estimate other parameters such as the critical bed depth **[24].** The critical bed depths estimated in our study were equal to 15.23 and 7.98 cm for 1 and 20% breakthrough, respectively. The rate constants calculated from the BDST graph intercept characterize the transfer rate of the solute from the liquid to the solid phase **[51].** For this system, the high values found for the determination coefficient and the N_0 adsorption potential justify the high efficiency of the laterite fixed-bed intercalated with activated carbon.

Preprints (www.preprints.org) | NOT PEER-REVIEWED | Posted: 14 September 2023 doi:10.20944/preprints202309.0972.v1

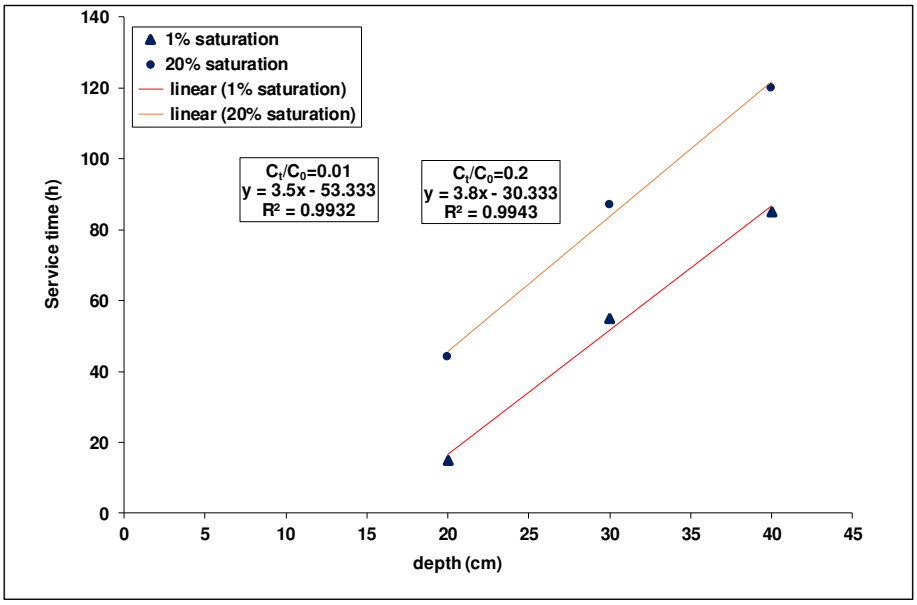

Figure 10. Evolution of service time "BDST"as a function of different bed heights (C_t = 1% C_0 and 20%C_0).

Table 8. Bed depth service time (BDST) model parameters.

C_t	Z_0 (cm)	N_0 (mg/L)	k_t (L/mg.h)	R^2
1%C_0	15.230	1335.600	11.600	0.993
20%C_0	7.980	1450.080	6.600	0.994

3.4.4. Effect of the initial concentration of As(III) on the breakthrough curve

Since the arsenic content in borehole waters present in the country is not constant, it is therefore necessary to investigate the influence of the initial *As(III)* concentration on the percolation process **[52]**. In order to establish the optimal performance of the continuous fixed-bed system, the effect of the *As(III)* initial concentration was studied by varying the concentration from 0.5 to 2 mg/L at a fixed flow rate of 50 mL/min and a bed height of 40 cm**. Figure 11** shows that the adsorbent adsorption efficiency decreased with the gradual increase of the arsenic concentration in the influent. For example, the breakthrough times were 32, 85 and 247 h for 2, 1, and 0.5 mg/L of *As(III)* concentration, respectively. Similarly, the volume of treated water decreased from 741 to 96 L as the inlet *As(III)* concentration increased from 0.5 to 2 mg/L. The possible explanation for these results is that higher concentrations in the influent may lead to a more rapid mass transfer and the increase of the water's ionic strength, allowing a rapid diffusion of arsenites onto the adsorbent surface **[53].** Consequently, a high concentration of arsenic in the tributaries leads to a reduction in the saturation time of the adsorbent **[53]**. In **Table 9**, we noted that when the initial concentration of *As(III)* at the inlet increased from 0.5 to 2 mg/L, the total amount of *As(III)* adsorbed (Q_{tot}) decreased from 295.362 to 191.011 mg and the mass retention capacity (Q_p) decreased from 0.165 to 0.107 mg/g. A high concentration of *As(III)* provides a great driving force to overcome the fixed-bed column mass transfer resistance **[54]**. In this context, it is suggested that the adsorption sites were almost covered when the concentration of *As(III)* increased **[54].** These results showed that a change in concentration gradient affected substantially the saturation rate and the breakthrough time **[15]**.

Preprints (www.preprints.org) | NOT PEER-REVIEWED | Posted: 14 September 2023 doi:10.20944/preprints202309.0972.v1

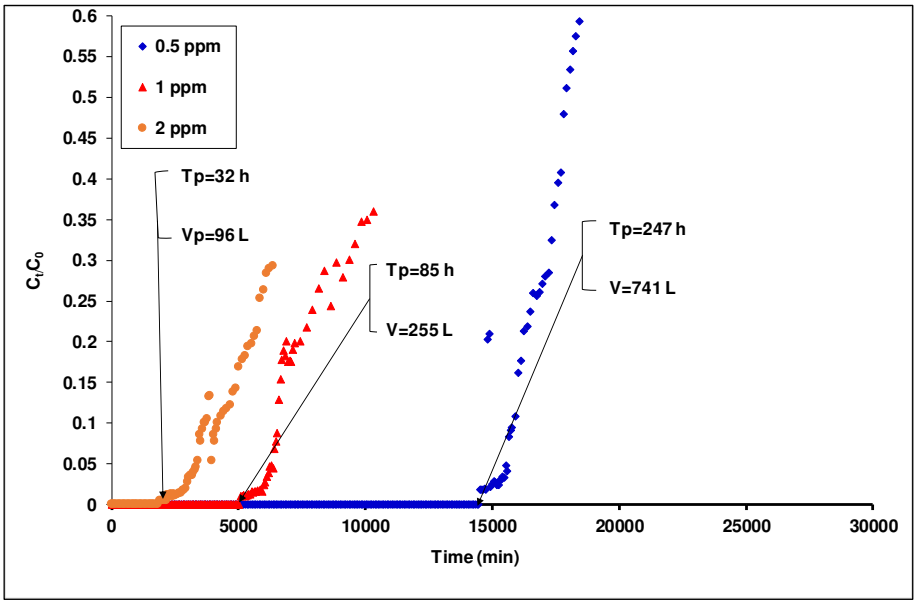

Figure 11. Breakthrough curves of *As(III)* adsorption in laterite packed column intercalated with activated carbon at different concentrations (Bed depth Z = 40cm, flow rate = 50mL/min; diameter =7cm; 0.900 ≤ G ≤ 1.250 mm).

Table 9. Fixed-bed column parameters for *As(III)* adsorption in DA laterite packed column intercalated with activated carbon at different concentrations.

C_0 (mg/L)	Q (mL/min)	Z (cm)	Mass(kg)	t_p (min)	V_p (L)	Q_{tot}(mg)	Q_p(mg/g)	R(%)
0.5	50	40	1.780	14820	741	295.362	0.165	99
1	50	40	1.780	5100	255	252.450	0.141	99
2	50	40	1.780	1920	96	191.011	0.107	99

3.4.5. Comparison of adsorption capacities obtained for the column packed with DA laterite intercalated with activated carbon (current study) with those reported in the literature.

This study investigated the removal of *As(III)* in a fixed-bed adsorption process using a column packed with DA laterite layers intercalated with BA-AC layers. The obtained results clearly showed that the column packed with laterite layers intercalated with BA-AC layers permitted to avoid the column clogging by laterite particles. Moreover, the process has the advantage of being applied for arsenic removal in real waters because of its ability to be adapted to multiple processes, which can reduce treatment and operating costs. A comparison between this study and other studies, reported in the literature on fixed-bed columns for arsenic adsorption, is summarized in **Table 10**. From this table, it can be noted that the issue of column clogging by laterite particles in a fixed-bed column is envisaged for the first time in our study. It is also noted that the application of the alternating layer technique is a promising technique with a relatively high breakthrough time compared to other reported works **[23,55,56].** A comparison of the Bohart-Adams adsorption capacity obtained in this study with those reported for other laterite adsorbents indicates that alternating DA laterite between BA-AC layers provided a higher adsorption capacity. According to Adam's modeling, to reach a maximum bed adsorption capacity (N_0) of 1335.6 mg/L of *As(III)* at 1% breakthrough, a minimum critical bed depth of 15.23 cm is required. The modeling data are experimentally meaningful for a pilot treatment unit design. The optimal conditions for an efficient removal of *As(III)* are as follows: a minimum depth of Z_{min} value set at 15.23 cm with an intercalation activated carbon height of 25 %, a granulometry of laterite ranging from 0.4 and 0.9 mm and an adsorbent dose of *As(III)* ranging from 0.5 to 2 mg/L. It is anticipated that the data obtained at the laboratory scale may provide useful data that can be accurately applied in domestic and industrial systems.

Preprints (www.preprints.org) | NOT PEER-REVIEWED | Posted: 14 September 2023 doi:10.20944/preprints202309.0972.v1

Table 10. Comparison of adsorption capacities obtained in the present study (column packed with DA laterite intercalated with activated carbon) with those reported in the literature.

Adsorbent	Clogging	Adsorbat	Initial concentration (mg/L)	The minimum depth *Zmin* (cm)	Adsorption capacity (mg/L)*	T_P(h)	References
Laterite soil	-	*As*	0.33	-		6.75	[57]
Natural Laterite (NL)	-	*As(V)*	1.00	9.11	67.00	24.00	[58]
Laterite soil	-	*As(III)*	0.50	-	108.02	32.00	[55]
Natural rocks coated with iron oxide (IOCNR)	-	*As(III)*	0.60	9.20	426.55	63.00	[56]
Natural laterite (NLTT)	-	*As(V)*	0.50	-	-	-	[23]
DA Laterite	Clogging reported	*As(III)*	1.00	-	-	-	Present study
DA Laterite + BA-AC	-	*As(III)*	1.00	15.23	1335.60	85.00	Present study

*Adsorption capacity corresponding to the minimum depth $Z_{min.}$

4. Conclusion

Adsorptive removal of *As(III)* through a laterite fixed-bed column intercalated with activated carbon layers, synthesized from *Balanites aegyptiaca* kernels, was performed with a good efficiency. Permeability data measurement allowed us to assess the intercalation of the adsorbent layers. The adsorption of *As(III)* depended strongly on the initial concentration of *As(III)* and the bed height. The parameters of the fixed-bed column were studied to find the optimal experimental operating conditions. Adsorption experiments on the laterite fixed-bed column allowed us to confirm that bed depth and particle size induced clogging of the column by laterite particles. In contrast, column clogging was not dependent on inlet concentration and flow direction. Investigating the effects of initial concentration and bed height, we found that breakthrough time decreased by raising the initial concentration and increased with the bed height. Modeling of the breakthrough curves by the Bohart-Adams model indicated a good fit to the experimental data. Indeed, based on the Bohart-Adams equation, the BDST model was used to predict the relationship between operating time and bed height, which is essential in the design of the column adsorption process. The Bohart-Adams model was found to be highly representative. The BDST model, which was used to evaluate the column design parameters, showed a good compliance with the experimental data. These results are a step towards the large-scale use of this type of laterite-filled column intercalated with activated carbon to provide cleaner water in rural areas.

Author Contributions: Conceptualization, D.R.O., C.B., A.K.S., B.S. and B.G.; Methodology, D.R.O., C.B., A.K.S., B.S. and B.G.; Investigation, D.R.O and C.B.; Writing—original draft preparation, D.R.O.; Writing—review and editing, D.R.O., C.B., A.K.S., B.S., B.G., A.L.H., E.Z., T.I.S., D.M., P.H and J.M.K.; Supervision, B.G., A.L.H., E.Z., T.I.S., D.M., P.H and J.M.K.; Funding acquisition, B.G., A.L.H., E.Z., T.I.S., D.M., P.H and J.M.K.; All authors have read and agreed to the published version of the manuscript.

Funding: The authors thank the ARES-CCD (Belgium), the Synergy 2018 project (Belgium) and the International Science Program (ISP, Uppsala, Sweden) for financial support.

Data Availability Statement: All data generated or analyzed during this study are included in this published article.

Acknowledgments: The authors thank the ARES-CCD (Belgium), the Synergy 2018 project (Belgium) and the International Science Program (ISP, Uppsala, Sweden) for financial support.

The authors thank Dr. François OUEDRAOGO for helpful discussion regarding the measurement of hydraulic conductivity.

Conflicts of Interest: The authors declare no conflict of interest.

References

1. Nasir, M.; Muchlisin, Z.A.; Saiful, S.; Suhendrayatna,S.; Munira,M.; Iqhrammullah,M. Heavy Metals in the Water, Sediment, and Fish Harvested from the Krueng Sabee River Aceh Province, Indonesia. *J. Ecol. Eng*., 2021, 22(9), 224 –2 31.
2. Khairunnash,A.;Muhammad ,I.;Rayyan,R.D.;Aulia ,A.;Qisthi ,M.A.; Agnia ,P.;Intan ,Q.; Kana,A.S.N.P. Heavy Metal Contamination in Aquatic and Terrestrial Animals Resulted from Anthropogenic Activities in Indonesia. *A Review*.2022, 1 – 8.DOI: 10.3233/AJW220049.
3. Glodowska ,M.; Stopelli ,E.; Thi ,D.V.; Pham ,T.K.T.;Pham ,H.V.;Michael ,B.;Andreas,K.; Sara,K. Arsenic behavior in groundwater in Hanoi (Vietnam) influenced by a complex biogeochemical network of iron, methane, and sulfur cycling. *J Hazard. Mater*.2020, 1-15. DOI: org/10.1016/j.jhazmat.2020.124398.
4. Liu, F.;Yang,W.;Li,W.; Zhao,G.C. Simultaneous oxidation and sequestration of arsenic(III) from aqueous solution by copper aluminate with peroxymonosulfate: a fast and efficient heterogeneous process. *ACS Omega*. 2021, 6(2), 1477–1487, DOI: org/10.1021/acsomega.0c05203.
5. Thangavel ,S.;Balarama ,V.;Mullapudi ,K.;Kora,A.J.;Kumar,S. Covellite (CuS) as a Novel Adsorbent for the Direct Removal of As (III) and As (V) Simultaneously from Groundwater. *Separation Sci and Technol*. 2021, 00 (00), 1–15. DOI: org/10.1080/01496395.2021.1944210.
6. Sakira,A.K.;Some ,T.;Ziemons ,E.;Dejaegher ,B.;Mertens ,D.; Hubert,P.;Kauffmann,J.M. Determination of arsenic (III) at a nanogold modified solid carbon paste electrode. *Electroanalysis.* 2015, 309–316. DOI: org/10.1002/elan.201400485.
7. He, X.;Deng ,F.;Shen ,T.;Yang ,L.;Chen ,D.;Luo ,J.;Luo ,X.;Min ,X.;Wang,F. Exceptional adsorption of arsenic by zirconium metal-organic frameworks: engineering exploration and mechanism insight. *J. Colloid Interface Sci.*2019, 539 ,223–234. DOI: org/10.1016/j.jcis.2018.12.065.
8. Ceballos-Escalera,A.; Pous ,N.; Chiluiza-Ramos ,P.;Korth ,B.;Harnisch ,F.; Bañeras ,L.;Balaguer ,M.D.;Puig,S. Electro-bioremediation of nitrate and arsenite polluted groundwater.*WaterRes*,190(2021),1-10,2021.DOI:org/10.1016/j.watres.2020.116748.
9. Garbinski, D.; Rosen, B.P.;Chen,J. Pathways of arsenic uptake and efflux. *Environ. Int*.2019,126, 585–597. DOI:org/10.1016/j.envint.2019.02.058
10. Gong, X.J.; Li,Y.S.; Dong,Y.Q.;Li,W.G. Arsenic adsorption by innovative iron/calcium in-situ-impregnated mesoporous activated carbons from low-temperature water and effects of the presence of humic acids. *Chemosphere.* 2020,250(126275),1-38 . DOI:org/10.1016/j.chemosphere.2020.126275
11. 11 Alka,S.;Shahir,S.; Ibrahim,N.;Ndejiko,M.J.;Vo,D.V.N.;Manan,F.A. Arsenic removal technologies and future trends: A mini review. *J. Clean. Prod*.2021,278, 1-14. DOI: org/10.1016/j.jclepro.2020.123805.
12. Türkmen ,D.;Türkmen , M.Ö.; Akgönüllü,S.;Denizli ,A. Development of ion imprinted based magnetic nanoparticles for selective removal of arsenic (III) and arsenic (V) from Wastewater. *Separ Sci Technol*.2021,00 (00),1–10. DOI : org/10.1080/01496395.2021.1956972.
13. Li, Y.; Zhu,Y.; Zhu,Z.; Zhang,X.; Wang,D.;Xie,L. Fixed-bed column adsorption of arsenic(V) by porous composite of magnetite/hematite/carbon with eucalyptus wood microstructure. *J. Environ. Eng. Landsc. Manag*.2018,26 (1), 38–56. DOI: org/10.3846/16486897.2017.1346513
14. Rahmi,R.;Lelifajri ·,L.; Iqbal ·,M.; Fathurrahmi,F.; Jalaluddin,J.;Sembiring,R.; Farida ·,M.; Iqhrammullah,M. Preparation, Characterization and Adsorption Study of PEDGE-Cross-linked Magnetic Chitosan (PEDGE-MCh) Microspheres for Cd2+ Removal.*Arab. J. Sci. Eng.*2022,1(48), 159–167.
15. Mahatheva ,K.; Loganathan ,P.;Vinh,T.;Nur,T. Iron-Impregnated granular activated carbon for arsenic removal : application to practical column fi lters. *J. Environ Man*.2019 ,239, 235–243. DOI: org/10.1016/j.jenvman.2019.03.053.–
16. Ramirez-Muñiz ,K.;.Perez-Rodriguez,F.;Rangel-Mendez,R. Adsorption of arsenic onto an environmental friendly goethite-polyacrylamide composite . *J Molecul Liq*.2018,264, 253–260 .DOI: org/10.1016/j.molliq.2018.05.063.
17. Andrea,M.;Franco ,D.E.;Carvalho ,D.B.C.; Bonetto ,M.M.;Roares,P.D.;Féris,L.A. Diclofenac removal from water by adsorption using activated carbon in 2 batch mode and fixed-bed column: isotherms,

thermodynamic study and breakthrough curves modeling . *Journal of Cleaner Production*.2018,6526(18),1-32. DOI: org/10.1016/j.jclepro.2018.01.138.

18. Chatterjee ,S.;Mondal,S.;De,S. Design and scaling up of fixed-bed adsorption columns for lead removal by treated laterite. *J. Clean Prod*.2018,177(7),60–74. DOI: org/10.1016/j.jclepro.2017.12.249.
19. Qu ,J.;Song ,T.;Liang ,J.;Bai ,X.;Li ,Y.;Wei ,Y.;Huang,S.; Dong,L. Ecotoxicology and environmental safety adsorption of lead (Ⅱ) from aqueous solution by modi fi ed auricularia matrix waste : A Fi Xed-Bed Column Study. *Ecot Environ Safety*.2019,169 , 722–729.DOI: org/10.1016/j.ecoenv.2018.11.085.
20. Huang ,Y.;Wang ,M.;Gong,Y.;Zeng,Y.E. Science of the total environment efficient removal of mercury from simulated groundwater using thiol- modified graphene oxide / femn composite in fixed-bed columns : experimental performance and mathematical modeling . *Sci Total Environ*.2020, 714 (136636),1-10. DOI: org/10.1016/j.scitotenv.2020.136636.
21. Hethnawi ,A.;Alnajjar ,M.;Manasrah ,D.A.; Hassan ,A.;Vitale ,G.; Jeong,R.; Nassar,N.N. Metformin removal from water using fixed-bed column of silica-alumina composite. *Colloids and Surfaces A*.2020, 597(124814), 1-12. DOI: org/10.1016/j.colsurfa.2020.124814.
22. Gupta,A.; Garg,A. Adsorption and oxidation of cipro floxacin in a fixed bed column using activated sludge derived activated carbon . *J Environ Man*.2019, 250(109474), 1-9. DOI: org/10.1016/j.jenvman.2019.109474.
23. Hai , N.T.;Thao ,A.;Loganathan,P.;Vinh ,T. Low-Cost laterite-laden household filters for removing arsenic from groundwater in vietnam and waste management. *Process Safety and Environ Prot*. 2021, 152, 154–163. DOI: org/10.1016/j.psep.2021.06.002.
24. Podder,M.S.; Majumder,C.B. Fixed-Bed column study for As(III) and As(V) removal and recovery by bacterial cells immobilized on sawdust / $MnFe_2O_4$ Composite. *Biochem Eng J*.2016,105, 114–135. DOI: org/10.1016/j.bej.2015.09.008.
25. Marian ,H.;Balintova,M.;Kovacova, Z.Evaluation of Zeolite Adsorption Properties for Cu (II) removal from acidic aqueous solutions. *In, Proceedings*.2018, 3–6. DOI: org/10.3390/proceedings2201293.
26. Boni, M.R.;Marzeddu,S.;Tatti,F.; Raboni,M.; Mancini,G.; Luciano,A.; Viotti,P. Experimental and Numerical Study of Biochar Fixed Bed Column for the Adsorption of Arsenic from Aqueous Solutions. *Water*.2021,13(915). DOI:org/10.3390/w13070915
27. Aline, A.L.; Neves, K.; Quina ,M.J.; Gando- Ferreira,M.L. Experimental and mathematical modeling of Cr(III) sorption in fixed-bed column using modified pine bark . *J. Clean Prod*.2018 ,1-28. DOI : 10.1016/j.jclepro.2018.02.094.
28. Ouedraogo, D.R. ; Bakouan, C. ; Sorgho, B. ; Guel ,B. Caractérisation d'une latérite naturelle du Burkina Faso En Vue de l 'élimination de l'arsenic (III) et l'arsenic (V) dans les eaux souterraines. *Int. J. Biol. Chem. Sci*.2019,13(6),2959-2977. DOI : 10.4314/ijbcs.v13i6.41.
29. Bakouan, C. Caractérisation de quelques sites latéritiques du Burkina Faso : application à l'élimination de l'arsenic (III) et (V) dans les eaux souterraines . Thèse de doctorat en cotutelle entre l'Université Ouaga I Pr JKZ et de l'Université de Mons. 2018, p.241.
30. Gul, A.; Hruza,J.;Yalcinkaya,F. Fouling and chemical cleaning of microfiltration membranes: A mini-review. *Polymers (Basel)*.2021,13(6),1-25. https://doi.org/10.3390/polym13060846.
31. Jeong, H.Y.; Jun,S.C.; Cheon, J.Y.; Minji,P. A review on clogging mechanisms and managements in aquifer storage and recovery (ASR) applications. *Geosci J.* 2018,22, 667–679. https://doi.org/10.1007/s12303-017-0073-x.
32. Bali, M. "Influence de l'aération Du Massif Filtrant Sur Les Performances Épuratoires Du Procédé d'infiltration-Percolation". *Rev Des Sci de l'eau*.2019, 31(4), 365–375. DOI : org/10.7202/1055594ar.
33. Karki, S.; Timalsina ,H.;Budhathoki,S.; Budhathoki ,S. Arsenic removal from groundwater using acid-activated laterite. *Groundw. Sustain. Dev*.2022. 100769 (18). DOI: org/10.1016/j.gsd.2022.100769
34. Wang, Y.; Liu, H.; Wang, S.; Li, X.; Wang, X.; Jia, Y. Simultaneous removal and oxidation of arsenic from water by δ-MnO_2 modifie activate carbon . *J. Environ Sci*.2020,94, 147–160. DOI: org/10.1016/j.jes.2020.03.006.
35. Nikié, J.; Agbaba, J.; Watson, M.A.; Tubié, A.;Šolić,M.;Maletié,S.; Dalmacija ,B. Arsenic adsorption on Fe–Mn modified granular activated carbon (GAC–FeMn): batch and fixed-bed column studies. *J. Environ. Sci. Heal. - Part A Toxic/Hazardous Subst. Environ. Eng*.201,54(3), 168–178. DOI:org/10.1080/10934529.2018.1541375

36. Meez,E.; Tolkou,A.K.; Giannakoudakis,D.A.; Katsoyiannis,I.A.; Kyzas,G.Z. Activated Carbons for Arsenic Removal from Natural Waters and Wastewaters . A Review" *Water*.2021,13(21), 29-82. DOI:org/10.3390/w13212982
37. Maazou, B.D.S.; Halidou ,I.H.;Mousbahou ,M.;Alma,M.; Adamou,Z. Elimination du chrome par du charbon actif élaboré et caractérisé à partir de la coque du noyau de *Balanites Aegyptiaca* élimination of the chromium by the élaborate activated coal and characterized from the c-ockle of the core of balanites aegyptiaca . *Int. J. Biol. Chem. Sci*.2017,11(6),3050-3065. DOI: 10.4314/ijbcs.v11i6.39
38. Essis, A.; Yao, Y.A.; Yao, K.U.; Albert, T. Optimisation de la préparation de charbons activés à base d'épis de maïs et caractérisation physico chimique [Optimization of the preparation of activated carbon based on corn cobs and physico-chemical characterization. *Int. J. Innov. Appl. Stud*.2020, 29(4), 1161–1171.
39. Clotaire, M. ; Avom , J. Pearwood (Baillonella Toxisperma Pierre) and Tested by Iodine évaluation des propriétés de charbons actifs de résidus de moabi (baillonella toxisperma pierre) par adsorption d ' iode en solution aqueuse. *J. Water Sci*.2019,29 (1), 51–60. DOI : org/10.7202/1035716ar
40. Basu, M. ; Guha, A.K. ; Ray, L. Adsorption of Lead on Lentil Husk in Fixed Bed Column Bioreactor. *Bioresour. Technol*, 283(2019):86–95,2019. https://doi.org/10.1016/j.biortech.2019.02.133
41. Ha, H.T.; Phong, P.T.; Minh, T.D. Synthesis of Iron Oxide Nanoparticle Functionalized Activated Carbon and Its Applications in Arsenic Adsorption. *J. Anal. Methods Chem.*2021 ,1-9. DOI:org/10.1155/2021/6668490.
42. Kundu, S.; Gupta,A.K. Analyse et modélisation du fonctionnement des colonnes à lit fixe sur l'élimination de l'As(V) par adsorption sur du ciment revêtu d ' oxyde de fer (IOCC). 2018,1,1–23. DOI : org/10.1016/j.jcis.2005.04.006
43. Sruthi, P.;Reddy,P. Effect of Alkali Concentration on Swelling Characteristics of Transformed Kaolinitic . Clays Clay Miner.2020, 68, 373–393. DOI:org/10.1007/s42860-020-00081-x.
44. Nguyen, T.A.H.; Ngo, H.H.H.; Guo, W.S.; Nguyen, T.T.; Vu,N.D.; Soda,S.; Nguyen,T.H.H.; Nguyen,M.K.; Tran,T.V.H.; Dang,T.T.; Nguyen,V.H.; Cao ,T.H. White hard clam (Meretrix lyrata) shells as novel filter media to augment the phosphorus removal from wastewater. *Sci. Total Environ*,2020,741(2020), 1-43.DOI: org/10.1016/j.scitotenv.2020.140483
45. Vieira, W. T.; Bispo, M.D.; Farias,S.D.M.;A meida,A.D.S.V.D.;Silva,T.L.D.;Vieira ,M.G.A.; Soletti ,J.I.; Balliano,T.L. Activated carbon from macauba endocarp (Acrocomia aculeate) for removal of atrazine: Experimental and theoretical investigation using descriptors based on DFT. *J. Environ. Chem. Eng*.2021,9 (2021),105-155. DOI: org/10.1016/j.jece.2021.105155
46. Rawat, S.; Maiti, A. A hybrid ultrafiltration membrane process using a low-cost laterite based adsorbent for efficient arsenic removal. 316(2023):1376-85,2023. DOI:org/10.1016/j.chemosphere.2022.137685.
47. KALENDA, G.M. Comportement des sols latéritiques compactés dans les remblais et digues de retenue des rejets miniers du Katanga (RDC). Thèse de doctorat à l'Université Catholite de Louvain. 2014, p.275.
48. Carneiro, M. A.;Pintor, A. M.A.; Boaventura, R.A.R.; Botelho, C.M.S. Efficient removal of arsenic from aqueous solution by continuous adsorption onto iron-coated cork granulates. 2022 ,432(128657),1-12. DOI:org/10.1016/j.jhazmat.2022.128657
49. Pantié,K.; Bajié,Z.J.; Veličković,Z.S.; Nešié,J.Z.; Đolié,M.B.; Tomié,N.Z.; Marinkovié,A.D. Arsenic removal by copper-impregnated natural mineral tufa part II: a kinetics and column adsorption study. *Environ. Sci. Pollut. Res*.2019, 26(23),24143–24161. DOI :org/10.1007/s11356-019-05547-7.
50. Goel , J.;Kadirvelu ,K.;Rajagopal,C.;Kumar,V. Remova l of lead (II) by adsorption using treated granular activated carbon : batch and column studies . *J. Hazard Mater B125*. 2005,125,211–120. DOI: org/10.1016/j.jhazmat.2005.05.032.
51. *Vijayasri, K.; Tiwari,A.; Chaudhari,C.V. Fixed-bed Column Studies on Removal of As (V) by Radiation Grafted Polymer 'Chitosan-g-MAETC. Anal. Chem. Lett.2019, 9(4),486–503. https://doi.org/10.1080/22297928.2019.1656546*
52. Bretzler, A.; Nikiema ,J.; Lalanne ,F.;Hoffmanna,L.; Biswakarma ,J.; Siebenaller ,L.;Demange,D.;Schirmer ,M.;Hug,S.J. Arsenic removal with zero-valent iron filters in Burkina Faso: Field and laboratory insights. *Sci. Total Environ*.2020,737, 39-66.
53. Verma, L.; Singh, J. Removal of As(III) and As(V) from aqueous solution using engineered biochar: batch and fixed-bed column study . Int. J. Environ. Sci. Technol.2023,20 (2023), 1961–1980. https://doi.org/10.1007/s13762-022-03920-7

54. Hai, N.T.; Paripurnanda, S.R..; Kandasamy, L. J.; Nguyen, T.V.; Vigneswaran, S. Arsenic adsorption by low-cost laterite column: Long-term experiments and dynamic column modeling. 2022,160(2022),868-875. DOI:org/10.1016/j.psep.2022.03.010.
55. Zhang, Y.;Xiong ,L.;Xiu,Y.; Huang,K. Defluoridation in fixed-bed column filled with Zr(IV)-loaded garlic peel. *Microchem J.* 2018,1-46. DOI: org/10.1016/j.microc.2018.11.007.
56. Kumar, S.;Pal ,A.;Pal,T.; Adak,A. Modeling and fixed-bed column adsorption of as (III) on laterite soil . *J.Separation and Purification Technology* .2007,56 (2007), 284–290.DOI: org/10.1016/j.seppur.2007.02.011.
57. Maji, S.K. ; Kao,Y.;Wang ,C.;Lu ,G.;Wu,J.;Liu,C. Adsorption en lit fixe d 'As (III) sur des roches naturelles revêtues d'oxyde de fer (IOCNR) et application aux eaux souterraines contenant de l'arsenic réel. *J. de génie chimique*.2012,203(2012), 285-293.DOI : org/10.1016/j.cej.2012.07.033
58. 58 Kumar, S; Pal , A; Pal,T. Arsenic removal from real-life groundwater by adsorption on laterite soil . *J. Hazard Mater*.2008,151 (2008) 811–820. DOI: org/10.1016/j.jhazmat.2007.06.060.